Strahlenther Onkol (2022) 198:254–267
https://doi.org/10.1007/s00066-021-01873-3

ORIGINAL ARTICLE

Automated hybrid volumetric modulated arc therapy (HVMAT) for whole-breast irradiation with simultaneous integrated boost to lumpectomy area

A treatment planning study

Savino Cilla[1] · Carmela Romano[1] · Gabriella Macchia[2] · Mariangela Boccardi[2] · Livia P. De Vivo[2] · Vittoria E. Morabito[1] · Milly Buwenge[3] · Lidia Strigari[4] · Luca Indovina[5] · Vincenzo Valentini[5,6] · Francesco Deodato[2,6] · Alessio G. Morganti[3,7]

Received: 7 June 2021 / Accepted: 17 October 2021 / Published online: 12 November 2021

Abstract

Purpose To develop an automated treatment planning approach for whole breast irradiation with simultaneous integrated boost using an automated hybrid VMAT class solution (HVMAT).

Materials and methods Twenty-five consecutive patients with left breast cancer received 50 Gy (2 Gy/fraction) to the whole breast and an additional simultaneous 10 Gy (2.4 Gy/fraction) to the tumor cavity. Ipsilateral lung, heart, and contralateral breast were contoured as main organs-at-risk. HVMAT plans were inversely optimized by combining two open fields with a VMAT semi-arc beam. Open fields were setup to include the whole breast with a 2 cm flash region and to carry 80% of beams weight. HVMAT plans were compared with three tangential techniques: conventional wedged-field tangential plans (SWF), field-in-field forward planned tangential plans (FiF), and hybrid-IMRT plans (HMRT). Dosimetric differences among the plans were evaluated using Kruskal–Wallis one-way analysis of variance. Dose accuracy was validated using the PTW Octavius-4D phantom together with the 1500 2D-array.

Results No significant differences were found among the four techniques for both targets coverage. HVMAT plans showed consistently better PTVs dose contrast, conformity, and homogeneity ($p < 0.001$ for all metrics) and statistically significant reduction of high-dose breast irradiation. V55 and V60 decreased by 30.4, 26.1, and 20.8% ($p < 0.05$) and 12.3, 9.9, and 6.0% ($p < 0.05$) for SWF, FIF, and HMRT, respectively. Pretreatment dose verification reported a gamma pass-rate greater than the acceptance threshold of 95% for all HVMAT plans. In addition, HVMAT reduced the time for full planning optimization to about 20 min.

Conclusions HVMAT plans resulted in superior target dose conformity and homogeneity compared to other tangential techniques. Due to fast planning time HVMAT can be applied for all patients, minimizing the impact on human or departmental resources.

The two authors Francesco Deodato and Alessio G. Morganti share the seniorship.

✉ Dr. Savino Cilla
savinocilla@gmail.com, savino.cilla@gemellimolise.it

[1] Medical Physics Unit, Gemelli Molise Hospital, Università Cattolica del Sacro Cuore, Largo Gemelli 1, 86100 Campobasso, Italy

[2] Radiation Oncology Unit, Gemelli Molise Hospital, Università Cattolica del Sacro Cuore, Campobasso, Italy

[3] Radiation Oncology Department, IRCCS Azienda Ospedaliero—Universitaria di Bologna, Bologna, Italy

[4] Medical Physics Unit, IRCCS Azienda Ospedaliero—Universitaria di Bologna, Bologna, Italy

[5] Radiation Oncology Department, Fondazione Policlinico Universitario A. Gemelli, Università Cattolica del Sacro Cuore, Roma, Italy

[6] Istituto di Radiologia, Università Cattolica del Sacro Cuore, Roma, Italy

[7] DIMES, Alma Mater Studiorum, Bologna University, Bologna, Italy

Keywords Autoplanning · Breast · Simultaneously integrated boost · Hybrid · Volumetric modulated arc therapy · Automation

Introduction

Adjuvant whole-breast radiotherapy after breast-conserving surgery is today the standard of care for early breast cancer patients [1]. Local control can be improved by an additional dose boost to the lumpectomy cavity after whole breast irradiation, providing significantly higher local control rates than whole breast irradiation alone in selected patients [2]. However, long-term follow-up studies reported radiation-related complications, such as breast fibrosis and pulmonary and/or cardiovascular toxicities, mainly due to inhomogeneous dose distributions [3, 4]. Also, the risk of developing contralateral breast cancer increases with the applied radiation dose, especially among younger patients, and also represents a serious concern to be considered when choosing an adequate treatment technique.

In the past few decades, a series of new techniques have been proposed aiming to achieve homogeneous dose distributions in order to decrease the rate of toxicity and improve cosmetic outcomes. Conventional tangential fields, usually consisting of two opposing wedged fields, are unsuitable for dose intensity modulation and dose inhomogeneities are usually unavoidable. Also, the use of wedges mainly contributes to dose scattering to the contralateral breast, increasing the risk of contralateral breast cancer. Thus, this technique has been mostly abandoned in modern radiotherapy. The so-called field-in-field technique has become a widely preferred method for tangential whole-breast radiotherapy, with several studies reporting better control of dose homogeneity [5]. This technique uses two open tangential photon beams and a small number of subfields, whose shapes and weights are manually determined to decrease hot-spot regions within the breast volume. However, this technique is very time-consuming and the results are to a high degree operator-dependent. The implementation of intensity-modulated techniques (IMRT), including the more recent volumetric modulated arc therapy (VMAT), translated in more homogeneous distribution and further reduction of lung and heart irradiation [6]. These new techniques also allowed for the simultaneous integrated boost (SIB), in which the dose boost is delivered to the tumor bed concurrently with whole breast irradiation, thus, avoiding overall treatment time prolongation, while exploiting the higher sensitivity of breast tumor cells to larger single doses [7]. This strategy demonstrated an improvement of tumor bed dose homogeneity and a decrease of normal tissue dose when compared to sequential boost [8, 9]. All the aforementioned advantages of IMRT techniques in terms of dose homogeneity and conformity are obtained at the cost of an increased low-dose bath to normal tissues, thus, representing a concern for the risk of developing second malignancies [10]. In particular, the use of VMAT for the irradiation of the left breast or chest wall is not yet widely accepted and the results of some dosimetric studies are very conflicting [11, 12]. Although controversial, the concerns related to the risk of an increase of radiation-induced secondary malignancies is still perceived as the major reason for limiting the widespread implementation of VMAT for whole breast irradiation [10].

A method to overcome these shortcomings is the use of a hybrid approach, in which the conventional 3D-CRT and IMRT/VMAT treatments are combined together, aiming to generate a good balance between homogenous dose distributions and robustness. In this technique, the higher percentage of the prescription dose (e.g., 70–80%) is delivered via tangential open beams without any modifiers, while the remaining dose (e.g., 20–30% of prescription dose) is delivered through a few IMRT fields or one or two partial VMAT arcs. IMRT fields or partial arcs are then optimized by the inverse planning engine in order to increase target dose homogeneity and coverage. The effectiveness of this technique has been investigated in a few studies, all reporting that the hybrid technique allows for higher dose uniformity across the breast, lower lung irradiation, and an easier and less complex planning procedure [13–15].

Despite the developments in radiation therapy planning over the past few years, the planning for left-sided whole breast irradiation may present several challenges to achieve clinically acceptable plans. Manually generated plans are usually obtained by an iterative procedure in which the planner continuously tunes the planning objectives in a trial-and-error procedure, until satisfactory dose distributions are achieved. This process is time-consuming and the final plan quality highly depends on the planner's experience [16]. Harmonization in radiotherapy treatment planning is therefore advisable for all patients to benefit from the high quality treatment independently of the planner skills or available time. Therefore, a well-designed automated planning strategy has the potential to improve current radiation oncology clinical workflow by standardizing plan quality and accelerating the treatment planning process.

Several semi-automated planning procedures were developed in order to improve the efficiency in breast radiotherapy, including the automatic selection of beam angles [17], the optimization of segment shapes and weights [18], and the use of scripting application programming interfaces to promote automation [19]. Recently, the Pinnacle treat-

ment planning system (Philips Medical Systems®, Fitchburg, WI, USA) introduced a new engine for fully automated optimization of the planning procedure. This engine, called Pinnacle Autoplanning, is a template-based planning optimization process engine using an iterative approach of progressive optimization that mimics all the steps of experienced and skilled planners without requiring any prior database of successful plans or model training [20]. With respect to breast treatments, Autoplanning has been recently tested for patients treated for accelerated partial breast irradiation [21], postmastectomy chest wall, [22], and whole breast cancer after breast-conserving surgery [23], in all cases reporting an improvement in target coverage and organs-at-risk dose sparing compared to manual treatment planning.

In the present paper, we described the implementation of the Autoplanning engine for breast cancer in a hybrid-VMAT strategy and compare plan quality with respect to several tangential techniques gradually implemented over time in our clinical practice. In particular, the hybrid-VMAT technique was optimized aiming to avoid the low dose-spread, typical of rotational techniques, partially mimicking tangential field irradiation. Then, we aimed to provide a practical protocol for the medical physicist and radiation oncologist community for the implementation of breast automated planning in clinical routine.

Materials and methods

Patient selection

Twenty-five consecutive patients with left-sided breast cancer (stage I/II, node negative) who underwent adjuvant radiotherapy after breast-conserving surgery were selected.

Simulation and volume definition

All patients were immobilized in supine position with the C-Qual TM Breastboard system (Civco Medical Solutions, Kalona, IA, USA), suitably designed for breast treatments. Computed tomography (CT) scans (Brilliance Big Bore, Philips, UK) was performed with slice thickness acquisition of 3 mm. The two clinical volumes (CTVs) include the breast (CTV_B) and the tumor bed (CTV_{TB}), the latter delineated on the basis of preoperative and operative reports and including the surgical clips and/or any surgery-induced changes considered to be a part of the lumpectomy cavity (hematoma or seroma). The corresponding PTVs, PTV_B and PTV_{TB}, were generated by expanding the CTVs by 5 mm, restricted 3 mm from external body. The normal organs included heart, ipsilateral lung, contralateral lung, and contralateral breast.

Treatment planning

All plans were created by two experienced medical physicists. For each patient four treatment plans were generated. The standard tangential wedged-fields (SWF), the field-in-field (FiF), and the hybrid-IMRT (HMRT) plans were generated using the Oncentra Masterplan treatment planning system (Elekta, Crawley, UK); the automated hybrid-VMAT (HVMAT) plans were generated using the Pinnacle TPS v.16.2 (Philips Healthcare, Fitchburg, WI, USA). In all cases, the collapsed cone algorithm was used for dose calculations with a dose calculation grid of 2 mm [24]. All plans were generated with a single isocenter placed at the center of the breast volume.

Prescribed doses were 50 Gy to the breast (PTV_B) in 2 Gy per fraction and a simultaneous integrated boost of 2.4 Gy per fraction to the tumor bed (PTV_{TB}). The dose requirements for both PTVs were based on the recommendations of ICRU Report 83 [25]**.** Objectives for target coverage of both PTVs were to treat 98% of the PTVs with an ideal of 95% of each prescription dose (i.e., 57.0 Gy for PTV_{TB} and 47.5 Gy for PTV_B). In addition, no more than 2% of the PTVs should exceed 107% of prescription doses.

For the heart, according to a recent international breast cancer randomized trial (NSABP B-51/RTOG1304), the main objective was to keep the mean dose below 4 Gy [26]. In addition, the objective V25Gy < 10% was also attempted since it has been associated with a < 1% probability of cardiac mortality 15 years after radiation therapy [27]. Following recent suggestions for the evaluation of radiation-induced lung toxicity [28], the objective for the ipsilateral lung were as follows: V5 < 50%, V20 < 20%, and V30 < 10% (V_X defined as the percentage of the total volume exceeding X Gy). The mean dose and D_{1cc} (dose to 1cc volume) to the contralateral breast was restricted to less than 2 and 5 Gy, respectively.

Details of the various techniques are described below.

Manual planning techniques

- *Standard tangential wedged technique (SWF)*

In this conventional planning technique, two parallel opposing tangential beams are used to ensure the best possible coverage of the breast target, minimizing the dose to the adjacent critical structures. Another similar couple of tangential beams are directed to the tumor bed. The "isocenter" of the treatment machine was positioned in the centroid of the breast. Dynamic wedges are added to tangential beams in order to improve the dose uniformity to the breast and tumor bed. Whenever possible, the central lung and heart distances were kept below 2.5 and 1 cm, respectively.

- *Tangential field-in-field technique (FIF)*

Forward-planned IMRT, also called field-in-field (FIF) is a practical technique in which one or more conformal segments are added to the tangential field [29, 30]. Two open tangential fields are created as for 3D-CRT technique, but without any beam modifiers, to include the whole breast. Equal weights are then assigned to these two open fields and the corresponding dose distribution is calculated. Since this configuration results in a large volume of underdosage in the thickest region of the breast, a second segment is defined to increase the dose to the deepest part of the breast while sparing the most superficial part. The MLC shape of this segment is defined on the basis of the dose cloud visualization from the previous large open fields, in order to cover with MLC dose level higher than 107%. In our experience, approximately 10% of the prescription dose was delivered with these reduced fields, while 90% of the dose is delivered by the primary tangents. A concomitant boost is subsequently generated for the tumor bed. Energy of beams was 6 MV for the primary open fields and 10 or 15 MV to the smaller segments, depending on maximum tangent separation.

- *Tangential hybrid IMRT technique (HMRT)*

The HMRT technique consisted of a conventional tangential-field plan and an inverse-planned IMRT plan. The 3D-CRT prescription (80% of total dose) was associated with a pair of open medial and lateral beams (with heart and lung MLC blocks), as for the FIF technique. The IMRT prescription (20% of total dose) was associated with two step-and-shoot beams using the same beam geometry as the 3D-CRT tangential beams. The energy of the beams was defined as explained for the FIF technique. Again, the medial and lateral open beams were set to be equal. The IMRT plan contribution was optimized by the Masterplan inverse-planning engine to supply the lacking dose, based on the following objectives: PTV1 uniform dose of 60 Gy, PTV1 $V_{57.0\,Gy} \geq 98\%$, PTV2 uniform dose of 50 Gy, PTV2 $V_{47.5\,Gy} \geq 98\%$, body maximal dose < 64.2 Gy, ipsilateral lung dose $V_{20Gy} < 10\%$, and mean heart dose < 4 Gy. A maximum total number of 10 segments was allowed (about 5 segments per beam) in order to reduce treatment time. The minimum segment area was set to 10 cm^2 to avoid the generation of segments that were too small. During this process, the optimization of 3D-CRT beams was set to "none" in the IMRT template.

- *Automated hybrid-VMAT technique (HVMAT)*

In this technique, two tangential fields plus a partial arc were integrated into a single treatment plan using the Autoplanning engine. Again, the actual dose weighting for the 3D-CRTcontribution was 80% of the prescribed dose and was used as the base plan. The Autoplanning module has been previously deeply described [20]. Briefly, it uses a user-defined template to automate a multiple sequence optimization process using a progressive optimization algorithm. The template contains all the beam parameters and dose and dose–volume goals for targets and organs at risk (OARs), including a tuning balance parameter which enables the user to tune the weighting between target coverage and OARs sparing and a dose fall-off margin parameter to improve the dose gradient around the PTVs. An example of technique used for breast cases optimization is presented in Fig. 1. The Autoplanning module is currently unable to manage a simultaneous optimization of mixed 3D-CRT/VMAT plans. In particular, the definition of beam set-up parameters for the 3D-CRT plan cannot be fully automatized in the technique and must be manually performed before the start of Autoplanning. The schematic diagram for HVMAT plan generation is shown in Fig. 2. The detailed process is described as follows. (1) A new case is presented

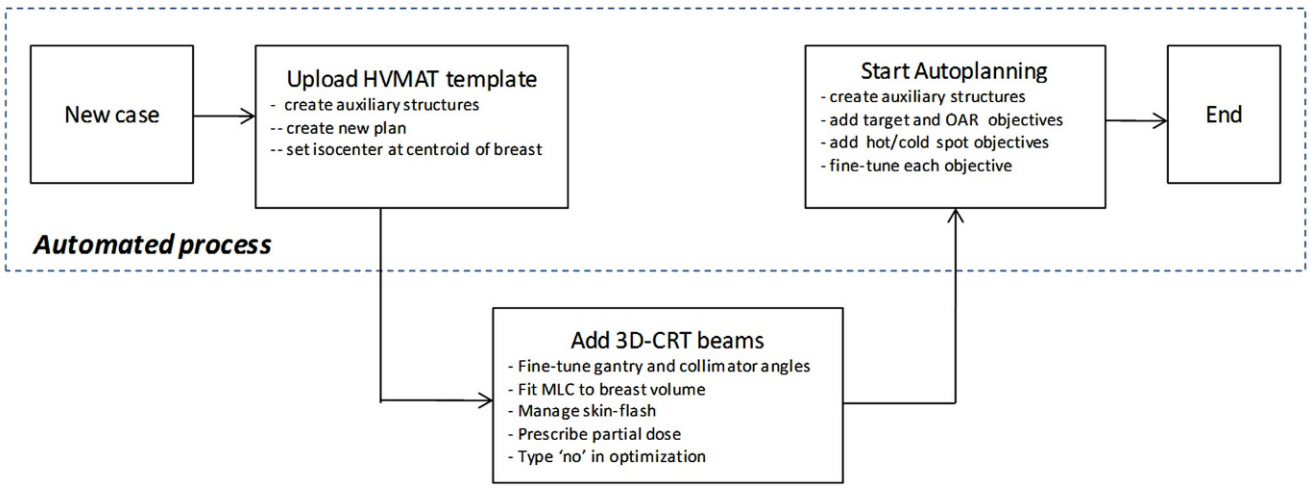

Fig. 1 Schematic diagram of HVMAT workflow. Detailed description is in the "Materials and methods" section

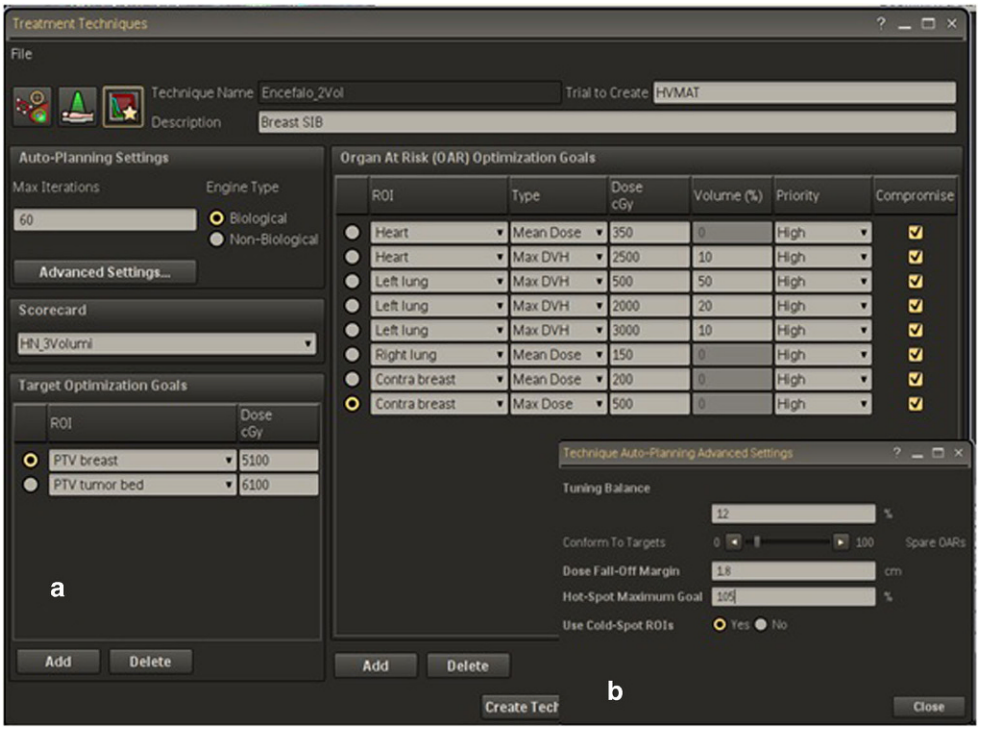

Fig. 2 **a** Autoplanning setup template for HVMAT techniquel, **b** advanced settings template

with completed contouring of targets and OARs. (2) Upload the HVMAT technique template. This automatically creates a new plan for a selected patient, sets the treatment isocenter in the centroid of the breast, creates a dummy volume for the whole breast to manage skin flash for the partial arc and presents to the planner the Autoplanning template (including all the preset definitions for arc length, energy, control point spacing, and dosimetric objectives). (3) In this template, add the two 3D-CRT tangential beams. This task is manually performed by identifying the optimal opposed tangential gantry angles and collimator angles for the selected patients, by fitting the MLC to the breast (including skin-flash) and prescribing the partial dose for the 3D-CRT contribution. Last, select the "none" option for the 3D-CRT beams in the optimization template, so the next optimization step will not involve the 3D-CRT beams. This manual task will take about 5 min. (4) Start Autoplanning. After the start of the optimization process, the Autoplanning engine automatically generates several dummy structures including: (a) rings around the PTVs to manage the dose fall-off, (b) residual targets structures where overlaps between no-compromised OARs are removed, (c) residual OARs structures where overlaps between targets are removed, (d) body structures used to control body dose and (e) hot-spot and cold-spot structures to manage target dose uniformity. New objectives are then automatically added to the aforementioned structures in order to achieve better OARs sparing and target uniformity and conformity for both PTVs. This process is iteratively performed during multiple optimization loops by adjusting the optimization parameters in order to continuously spare the OARs without compromising the target coverage, i.e., mimicking what a manual experienced planner would usually do. (5) The HVMAT plan is completed.

Five previous patients, not included in the present series, were used to tweak the initial technique in order to generate plans fulfilling the clinical objectives.

The optimization objectives for the OARs used in the treatment technique are reported in Fig. 2. All HVMAT were optimized using the following settings: tuning balance equal to 12%, dose fall-off margin equal to 1.8 cm, the hot-spot maximum goal equal to 105%, and the "Use Cold-Spot ROIs" option checked. The maximum number of iterations was set to 60.

Plan evaluation

Dose–volume histogram (DVH) analysis was used for plan comparison. The target volumes coverage were compared in terms of D98%, D95%, D50% and D2% (i.e., the doses to 98%, 95%, 50% and 2% of target volumes, respectively).

The dose conformity number (CN) was calculated for both PTVs, using the Van't Riet formula [31]:

$$CN = \frac{TV_{RI}}{TV} \times \frac{TV_{RI}}{V_{RI}}$$

Where TV_{RI} is the target volume covered by the reference isodose, TV is the target volume and V_{RI} is the volume

of the reference isodose. The two ratios define the quality of target coverage and the irradiation of healthy tissues at the prescription dose level. CN values range from 0 (complete PTV geographic miss) to 1 (perfect conformity of the reference isodose).

For each PTV, the homogeneity index (HI) was calculated as:

$$HI = \frac{(D2\% - D98\%)}{D_p}$$

where D_p is the prescription dose. The HI ideal value is 0.

As the delivery of simultaneous higher doses to the tumor bed increases the dose to the surrounding breast tissue, we analyzed the excess irradiation to the whole breast by different techniques by creating a new structure as the whole breast excluding the tumor bed, called PTV_M. Excess irradiation and overdosage of the whole breast was defined by the volume of PTV_M receiving more than 50, 55, and 60 Gy. The mean dose of PTV_M was also calculated for comparison purposes and for the definition of a new metric called dose contrast index (DCI) [32]. The ideal DCI (iDCI) is defined as the ratio between the prescription doses to the tumor bed and breast (i.e., in the present study by 60/50 = 1.2). The actual DCI is defined as the mean dose to the PTV_{TB} divided by the mean dose to the PTV_M. The ratio of DCI and iDCI will define the percentage DCI (%DCI) providing the deviation of the actual DCI from the ideal iDCI. A DCI value closer to 1 indicates a better dose contrast.

Dosimetric verification

A dosimetric verification was performed to assess the reliable deliverability of HVMAT plans. Plans were transferred to the Octavius-4D motorized cylindrical phantom, able to rotate synchronously with the gantry. Dose distributions were measured utilizing the 1500 2D ion-chamber array (PTW, Freiburg, Germany), a matrix of 1405 ion chambers inserted in the Octavius phantom, providing a three-dimensional dose reconstruction. The agreement between measured and calculated doses was defined by the γ index (global 3%/2 mm criterion). Dose verification was considered optimal if the percentage of points fulfilling γ index criteria exceeded 95%.

Statistical analysis

Statistical comparisons of data were performed by a Kruskal–Wallis analysis of variance followed by a Bonferroni–Dunn post hoc non-parametric test in order to correct for multiple comparisons. A *p*-value at 0.05 indicated statistical significance.

Results

Breast sizes varied from 191–1372 cm^3, with a median value of 571 cm^3. Similarly, tumor bed volumes ranged from 22–408 cm^3, with mean value of 99 cm^3.

PTVs coverage

Table 1 reports the dosimetric results for the PTV_{TB} and PTV_M.

All required criteria for targets coverage were met in all 100 generated plans. No significant differences were found in near-minimal doses (D98%) for both tumor bed and breast coverage between any techniques. On average

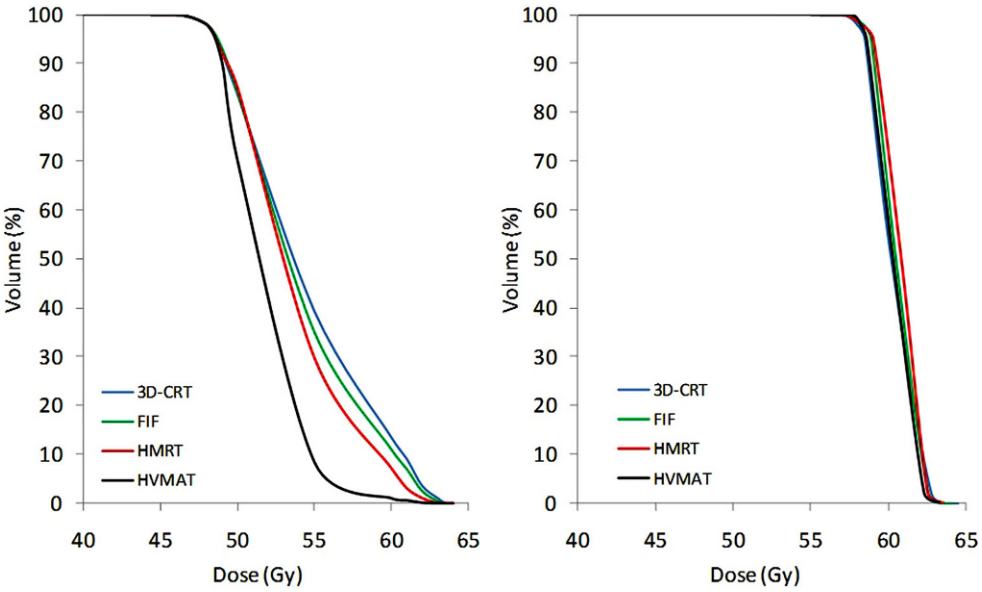

Fig. 3 Average cumulative dose–volume histograms for the tumor bed and the whole breast (excluding the tumor bed) comparing the 3D-CRT (*blue*), FIF (*green*), HMRT (*red*), and HVMAT (*black*) treatment techniques. *3D-CRT* Standard tangential wedged technique, *FIF* Tangential field-in-field technique, *HMRT* Tangential hybrid IMRT technique, *HVMAT* Automated hybrid-VMAT technique

Table 1 Comparison of target coverage metrics and dose conformity for the PTVs as a function of plan technique.

Structure	Metric	Objective	3D-CRT	FIF	HMRT	HVMAT	*p*	*p*		
							Kruskal–Wallis	3D-CRT vs. HVMAT	FIF vs. HVMAT	HMRT vs. HVMAT
PTV_{TB}	D98 (Gy)	≥ 57.0	58.0 ± 1.1	58.2 ± 0.8	58.2 ± 0.7	58.2 ± 0.7	0.951	0.633	0.957	0.926
	D50 (Gy)	60.0	60.2 ± 0.8	60.5 ± 0.6	60.6 ± 0.6	60.3 ± 0.2	0.088	0.672	0.142	0.088
	D2 (Gy)	≤ 64.1	63.0 ± 0.9	62.6 ± 0.7	62.5 ± 0.6	61.6 ± 0.3	**< 0.001**	**< 0.001**	**< 0.001**	**< 0.001**
	HI	Minimize	8.3 ± 2.0	7.3 ± 2.0	7.2 ± 1.8	5.7 ± 1.2	**< 0.001**	**< 0.001**	**< 0.001**	**< 0.005**
PTV_M	D98 (Gy)	≥ 47.5	48.0 ± 1.0	48.1 ± 0.8	48.1 ± 0.7	48.1 ± 0.7	0.955	0.755	0.777	0.861
	D50 (Gy)	50.0	54.5 ± 1.2	53.6 ± 1.2	53.3 ± 0.9	51.1 ± 0.4	**< 0.001**	**< 0.001**	**< 0.001**	**< 0.001**
	D2 (Gy)	≤ 53.5	62.8 ± 0.7	62.3 ± 0.6	61.6 ± 0.6	58.5 ± 0.5	**< 0.001**	**< 0.001**	**< 0.001**	**< 0.001**
	V55 (%)	Minimize	39.5 ± 13.8	35.2 ± 13.0	29.9 ± 9.6	9.1 ± 2.9	**< 0.001**	**< 0.001**	**< 0.001**	**< 0.001**
	V60 (%)	Minimize	13.4 ± 9.3	11.0 ± 6.8	7.1 ± 6.9	1.1 ± 0.1	**< 0.001**	**< 0.001**	**< 0.001**	**< 0.001**
	HI	Minimize	29.2 ± 4.1	28.2 ± 2.8	26.6 ± 1.8	22.0 ± 1.7	**< 0.001**	**< 0.001**	**< 0.001**	**< 0.001**
Dose conformity	CN_{TB}	1.0	0.23 ± 0.07	0.25 ± 0.07	0.34 ± 0.10	0.74 ± 0.06	**< 0.001**	**< 0.001**	**< 0.001**	**< 0.001**
	CN_M	1.0	0.46 ± 0.11	0.51 ± 0.11	0.51 ± 0.11	0.71 ± 0.08	**< 0.001**	**< 0.001**	**< 0.001**	**< 0.001**
Dose contrast index	DCI	100.0	92.8 ± 2.5	93.1 ± 2.5	94.0 ± 1.3	97.9 ± 0.9	**< 0.001**	**< 0.001**	**< 0.001**	**< 0.001**

Vx (%) is the percentage volume receiving X Gy. D1cc is the dose to 1cc volume. Dx (Gy) is the dose to x% volume, HI is the homogeneity index, CNs are the conformation numbers for the breast and tumor bed and DCI is the dose contrast index.

HVMAT plans decreased near-maximal doses (D2%) for the breast excluding the tumor bed by 5.8, 5.2, and 3.9% ($p < 0.05$) for the SWF, FIF, and HMRT techniques, respectively.

The median dose and the volume of PTV_M receiving more than 55 and 60 Gy were found to be significantly lower for the HVMAT plans. In particular, mean V55 and V60 decreased by 30.4, 26.1, and 20.8% ($p < 0.05$) and 12.3, 9.9, and 6.0% ($p < 0.05$) for the SWF, FIF, and HMRT techniques, respectively. These findings translated in a more homogenous dose distribution for HVMAT plans. This behavior is well highlighted in Fig. 3, reporting the average cumulative dose–volume histograms of all techniques for all patients for the tumor bed PTV_{TB} and the whole breast excluding the tumor bed PTV_M.

The isodoses distribution of all four treatment modalities for a representative patient is shown in Fig. 4.

Dose conformity

Dosimetric results for dose conformity are summarized in Table 1, and Fig. 5 shows the boxplots for the dose conformity indexes. HVMAT plans significantly improves the conformation numbers from 0.23 to 0.74 for the tumor bed and from 0.46 to 0.71 for the breast ($p < 0.05$). Similarly, the dose contrast index was strongly improved by 5.5, 5.2, and 4.1% ($p < 0.001$) for the SWF, FIF and HMRT techniques, respectively.

OARs sparing

The dosimetric findings for heart, left and right lungs and contralateral breast are reported in Table 2 and Fig. 6.

For ipsilateral lung and heart, no statistically significant differences were found for all reported dosimetric metrics (Table 2). With respect to contralateral lung, mean doses were found < 2 Gy for all techniques. For the contralateral breast, the mean doses were < 1 Gy for all techniques, with no significant differences. HVMAT provided the lower values for the near-maximal dose D1cc, with a mean significant decrease of approximately 1 Gy ($p < 0.05$).

Dosimetric verification

Pretreatment verification was performed for all HVMAT plans. With criteria equal to 3% (global)/2 mm for γ index, the average pass-rate was found 97.9% (range 95.8–100%) for all plans.

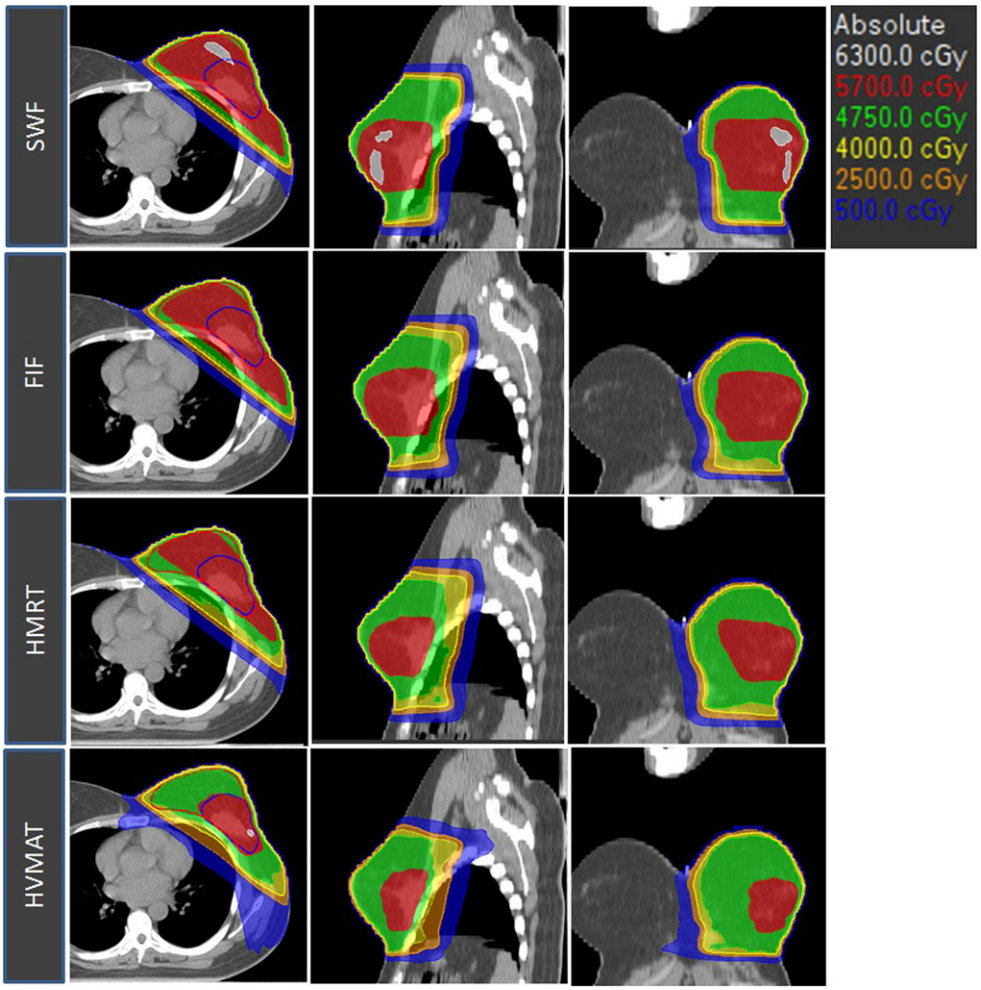

Fig. 4 Representative two-dimensional dose distributions in axial, sagittal and coronal planes for a representative patient. *SWF* conformal tangential wedged technique, *FIF* tangential field-in-field technique, *HMRT* hybrid-IMRT technique, *HVMAT* automated hybrid-VMAT technique

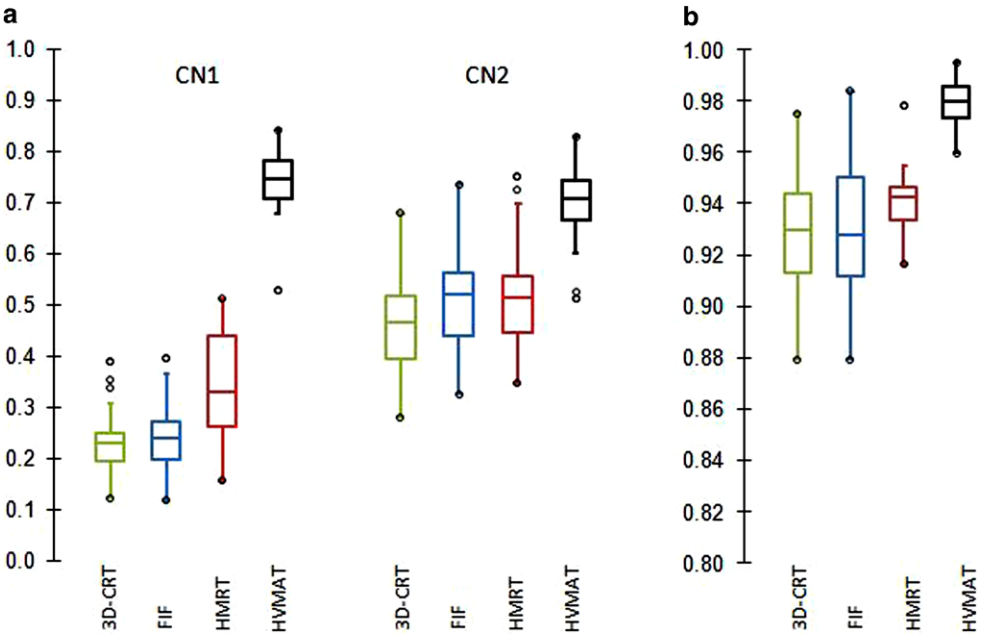

Fig. 5 Boxplots of dose conformity and dose contrast indexes for all techniques. **a** Dose conformity for both PTVs defined by Van't Riet formula, **b** dose contrast index (DCI)

Table 2 Comparison of normal tissue dose–volume metrics as a function of plan technique.

Structure	Metric	Objective	3D-CRT	FIF	HMRT	HVMAT	*p*	*p*		
							Kruskal–Wallis	3D-CRT vs. HVMAT	FIF vs. HVMAT	HMRT vs. HVMAT
Heart	Dmean (Gy)	<4	2.4 ± 0.8	2.4 ± 0.7	2.6 ± 1.0	2.6 ± 1.0	0.883	0.498	0.727	0.982
	V25 (%)	<10	1.5 ± 1.4	1.3 ± 1.2	1.7 ± 1.6	1.6 ± 1.4	0.883	0.706	0.423	0.762
Left lung	Dmean (Gy)	–	8.1 ± 2.1	7.4 ± 1.9	7.6 ± 1.8	7.1 ± 2.0	0.229	0.051	0.514	0.174
	V5 (%)	<50	26.1 ± 5.3	24.9 ± 4.7	25.8 ± 4.6	25.9 ± 6.4	0.566	0.738	0.304	0.893
	V20 (%)	<20	14.7 ± 4.3	13.1 ± 3.9	13.9 ± 3.8	13.8 ± 5.6	0.492	0.324	0.621	0.643
	V30 (%)	<10	12.7 ± 4.0	11.0 ± 3.5	11.6 ± 3.5	10.0 ± 4.8	0.099	**0.018**	0.425	0.103
Right lung	Dmean (Gy)	<2	1.7 ± 0.6	1.7 ± 0.5	1.7 ± 0.5	1.5 ± 0.5	0.199	0.203	0.073	0.053
Right breast	Dmean (Gy)	<2	0.6 ± 0.2	0.7 ± 0.2	0.7 ± 0.1	0.7 ± 0.2	0.057	0.144	0.203	0.450
	D1cc (Gy)	<5	5.0 ± 1.4	5.2 ± 1.3	5.3 ± 1.6	4.0 ± 1.7	**0.008**	**0.019**	**0.002**	**0.005**

Vx (%) is the percentage volume receiving X Gy. D1cc is the dose to 1cc volume

Discussion

Several investigations on the role of VMAT for breast radiotherapy has proven that, as a trade-off of more homogeneous and conformal dose distributions, a large volume of surrounding tissues would receive a low-dose bath [11, 12]. Although this was an expected feature of VMAT technique, the low-dose bath is still a concern for the increased risk of developing secondary malignancies, and many institutions are reluctant to implement a clinical widespread use of this technique for breast irradiation. Abo-Madyan et al. [33] calculated the excess absolute risk of a second cancer occurring after breast radiotherapy for different treatment techniques, reporting that second cancer risk after VMAT was found higher than for 3D conformal therapy by about 34% for the linear model and 50% for the linear–exponential and plateau models, respectively. This issue stimulated the exploration of alternative planning techniques to improve the disadvantages of pure-VMAT. In order to balance the respective advantages of 3D-CRT conformal and volumetric techniques, a so-called hybrid VMAT technique has been developed combining the two aforementioned techniques in a composite approach [14, 15]. On the other hand, efforts to streamline and standardize planning procedures using automated algorithms have been also pursued in the last few years.

Based on the aforementioned considerations, we hereby described the implementation of a hybrid VMAT technique with the added value of the automation of treatment planning, as an optimal class solution for left breast cancer irradiation in clinical routine. Then we retrospectively analyzed and compared the new automated HVMAT plans with three manually generated different techniques, which demonstrated that HVMAT improved the treatment planning workflow in terms of quality and efficiency. This technique has been recently implemented in our clinical practice for all breast treatments as the last step of our continuing efforts to improve plan quality and decrease potential toxicities in this clinical setting [34].

One of the main results of the present study is a major decrease of breast tissue receiving high doses. HVMAT reported significantly lower mean dose and volumes of the whole breast excluding tumor bed receiving more than 55 Gy, reporting a 30.8, 21.6, and 21.3% reduction in excess irradiation at the 110% dose level (55 Gy) for the 3D-CRT, FIF, and HMRT techniques, respectively. This is a relevant result with potential clinical significance because the risk of breast fibrosis has been reported to be influenced by the use of a boost dose to the tumor bed [2]. The EORTC 22881-10882 trial [2] investigated the long-term impact of a boost radiation dose of 16 Gy on local control, fibrosis, and overall survival for patients with stage I and II breast cancer who underwent breast-conserving therapy. Among the results, it was reported that severe fibrosis was significantly increased in the boost group, with a 10-year rate of 4.4% versus 1.6% in the no boost group ($P < 0.0001$). The significant reduction of excess irradiation to breast reported by HVMAT might also have relevant clinical implications in terms of better cosmetic outcome [35] and reduction of acute complication rate [36].

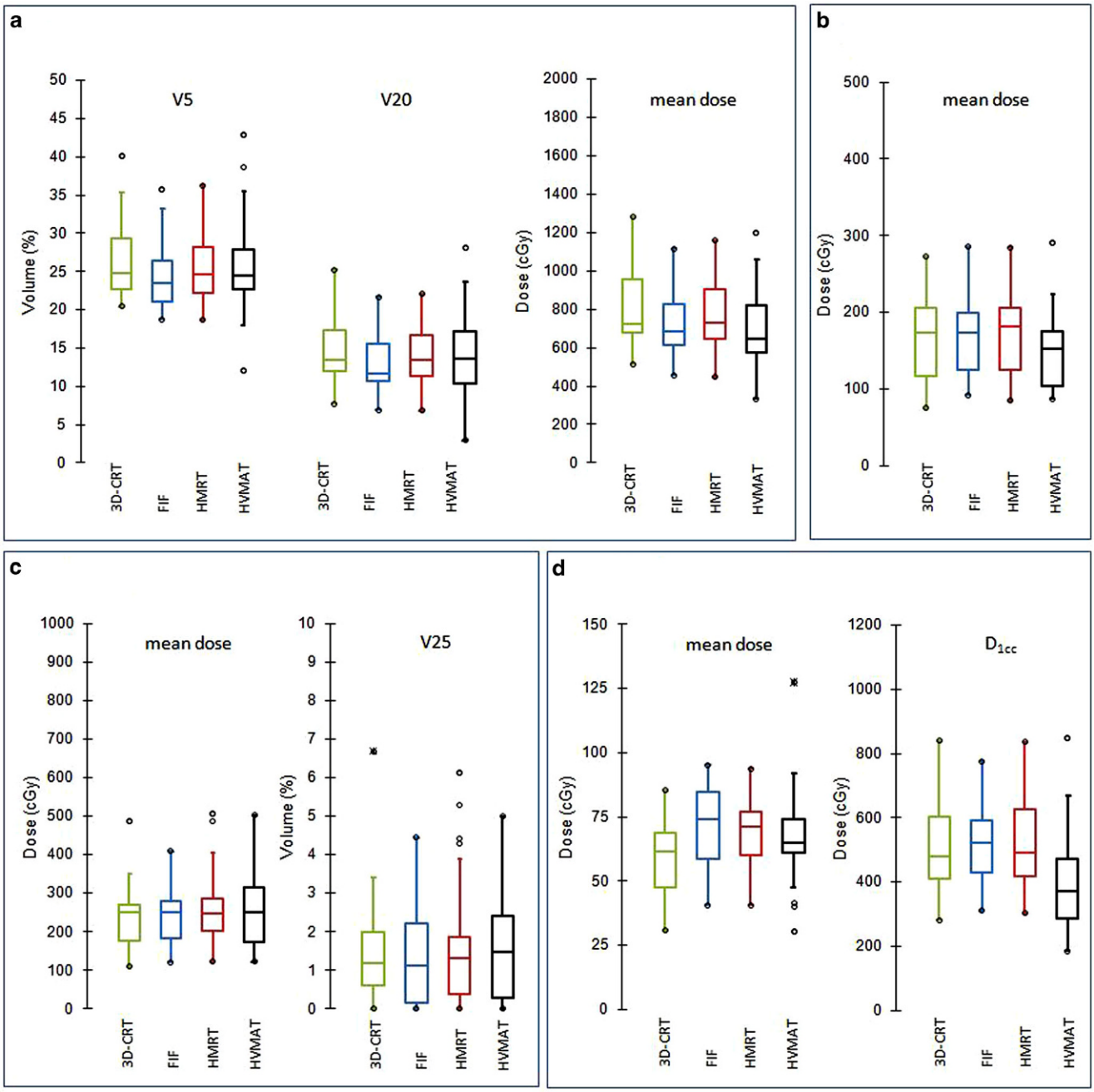

Fig. 6 Boxplots of main dosimetric metrics for organs at risk (OARs) for all techniques. **a** Left lung, **b** right lung, **c** heart, **d** right breast. *V5*, *V20* and *V25* are the volumes percentage receiving 5, 20 and 25 Gy, respectively. *D1cc* is the dose to 1cc volume.

With regard to normal tissue sparing, increasing attention has been focused in the last decade on the development of radiation-induced secondary cancer in the contralateral breast and lung. The WECARE study [37] aimed to quantify the risk of second primary breast cancer in the contralateral breast following radiotherapy for first breast cancer. The results highlighted that women <40 years of age who received >1 Gy to the contralateral breast had a 2.5-fold greater risk of developing a second primary cancer than unexposed women (95% confidence interval 1.4–4.5) and that the dose response was significant. In our study, a mean dose of 0.65 Gy was observed with HVMAT for contralateral breast, a value not significantly different with respect to the other techniques. In addition, HVMAT reported the lower mean value for near-maximal dose (D1cc), although not statistically significant. This findings suggest that HVMAT does not increases the contralateral breast cancer occurrence with respect to the other tangential techniques.

Grantzau et al. [38] reported a linear increased risk of second primary lung cancer 5 or more years after breast

irradiation by 8.5% per Gy. In particular, the adjusted risk of lung cancer was found greater than threefold for doses of 15 Gy. We reported a mean dose to ipsilateral lung with HVMAT of 7.7 ± 1.8 Gy, not significantly different with respect to the other three techniques. Unexpectedly, HVMAT was not associated with a low-dose bath to a large volume of ipsilateral lungs. This low-dose bath, here quantified by the V5Gy metric, was not found to be significantly different compared to other techniques. This is an encouraging achievement in the light of emerging evidence of lung V5 Gy as a predictor for pneumonitis [39]. In addition, we also reported the feasibility of HVMAT to keep the mean dose to the contralateral lung below 2 Gy for all patients, as for the other tangential techniques.

The increased risk of cardiac toxicity after breast radiotherapy has been investigated in depth in the last 2 decades. In particular, Darby et al. [40] reported a linear increase in risk of major coronary events by 7.4% per Gy in heart mean dose, using a model for increased risk with a threshold on mean heart dose of 3 Gy. Our results, as reported in Table 2 indicated HVMAT supplied a heart mean dose below 3 Gy and that the differences among the four techniques were within 0.3 Gy on average, so that the differences in cardiac risks of all four techniques would be considered negligible. In addition, the heart V25% was found to be around 2%, well below the Quantec guidelines [27] reporting that V25% < 10% is associated with a < 1% probability of cardiac mortality 15 years after radiation therapy. These results are consistent with the awareness that no known "safe" levels of dose to the heart have been proposed; therefore, the aim is to spare the heart as much as possible.

All HVMAT plans in this study were optimized with a technique delivering 80% of the dose with the open tangential fields to the breast and the remaining 20% with a VMAT half-arc. This choice is based on our previous experience with FIF and hybrid IMRT techniques [29] and was confirmed during the implementation process of HVMAT, when several mixtures of dose weights were tested. A recent study [15] aiming to find the optimal dose weighting for hybrid volumetric modulated arc therapy for left-sided chest wall and breast cancer confirmed our choice. In this study, a sequence of HVMAT plans were generated for 20 left breast patients, respectively, by combining different dose proportions of 3D-CRT and VMAT plans (from 90–10% to 50–50%). Compared with other proportions, 80% 3DCRT/20% VMAT weighted plans achieved the better balanced results, effective in reducing the low-dose volume without compromising the PTVs dosimetric parameters. This choice may limit the potential for optimization and partially explains the lack of major differences between the techniques, but our goals were more focused on risk reduction than in maximizing dose conformity to the boost region. In our opinion, this approach represents a good balance between homogeneity and minimizing the exposure of the organs at risk. This approach is nowadays supported by other authors [13–15, 41] and by the lack of clinical evidence for other techniques than tangential. In particular, while the role of full VMAT is now consolidated in in-silico studies, limited evidence has been presented in the literature from a clinical perspective.

A notable advantage of HVMAT technique is its higher robustness against geometrical uncertainties due to the high weight of dose to be delivered by open fields [42]. In fact, a challenging aspect of pure-VMAT delivery in breast cancer is the difficult management of plan robustness (in terms of inter- and intrafraction motion), particularly when significant breast swelling occurs during the treatment course. In particular full intensity-modulated plans optimized without a skin flash margin reported significant underdosage of the breast surface [42]. A few attempts [43] have been made to address the skin flash problem for the VMAT technique, including the use of a virtual bolus in the region of the PTV outside the external contour during optimization. However, plan degradation is inevitable upon removal of these dummy volumes for final dose calculation and additional manual optimization must be performed to regain plan quality. Thus, in order to improve the robustness in more complex techniques, it is necessary to increase the immobilization and setup accuracy not only through the use of image guidance but also with breath-hold or gating techniques [44]. Hybrid VMAT strongly mitigate this issue by incorporating skin flash in the field apertures of the 3D-CRT component, thus ensuring the irradiation of all breast tissue also in cases of respiratory-related motion or increased breast size compared to the planning CT. From this point of view, it must be highlighted that all patients in this study has been optimized without the use of breath-hold techniques, so that our strategy can be also applied to all centers lacking technology for breath control. An upcoming study is in its planning stage for the quantitative assessment of the robustness of HVMAT plans in this clinical setting.

Compared with other cancer sites, the planning procedure for whole breast irradiation is usually less complex. However, breast planning usually contributes to the larger proportion of the workload for dosimetrists, medical physicists, and radiation oncologists in most departments (about 25–30% of all patients). Breast cancer cases thus represent an ideal candidate to prioritize the implementation of full treatment planning automation to efficiently handle the most routine cases. In this study, automated HVMAT plans were generated in about 20 min. This result translated into a huge impact in terms of reduction of planning times in busy departments, so that a major improvement of planning efficiency must be expected. For example, in our radiation oncology department where about 250 breast patients are treated per year, a saved time of ≥ 300 h can be estimated per

year. In addition, the automation of treatment planning have also the potential to reduce interplanner variability (e.g., between experienced and non-experienced planners), as recently demonstrated for complex head–neck and prostate cancer cases [20].

A shortcoming of this hybrid approach for breast treatments is that the workflow process for Autoplanning should not be still considered a fully automated solution, contrary to what was demonstrated for other anatomical sites [20]. As reported in Fig. 1, after the loading of the HVMAT template, it is necessary to manually add the two 3D-CRT tangential beam in this template, fine-tune the directions of the fields according to the body habitus and the shape of PTV, provide the partial dose proscription and disable them from inverse-based optimization process. However, this operation takes place very quickly (less than 5 min) and the resulting procedure continues to allow each planner not to waste time on the tedious and repetitive parts of the planning process and commit more resources to more complicated cases.

Another limitation of this study is the failure in evaluating the doses to the cardiac substructures such as the left ventricle and the left descending artery, due to the use of non-contrast enhanced CT images. Indeed, there is an increasing evidence that the dose to these heart substructures needs to be considered in breast cancer planning in order to further radiation-related cardiotoxicity [45]. However, the routine use of non-contrast enhanced CT images prevents the accurate visualization and delineation of these structures, in addition to the impact of breathing, swallowing, cardiac motion, and set-up errors on the reliability of the dose distribution for such OARs. Therefore, in the present study the heart was considered a single organ and we adopted reliable guidelines for dose comparison purposes.

A final note of caution must be devoted to the use of different TPS in the present study. Despite the use of a different optimization engine for the HVMAT plans, all dose calculations were performed with the same algorithm, i.e., the collapsed cone convolution, and with the same dose calculation grid of 2 mm. This algorithm was investigated in depth on phantoms and clinical breast patients with different respiratory phases; the results were equivalent to MonteCarlo simulations and also in the peripheral dose calculation accuracy [46].

Conclusion

We developed an efficient automated procedure for HVMAT planning that was readily integrated into clinical practice. HVMAT technique produces high-quality plans using only a template-based procedure, with minimal human intervention. By retrospectively comparing the HVMAT plans with different manually optimized tangential techniques, we have shown that this strategy improves the treatment planning workflow in quality standardization and efficiency by eliminating the repetitive planning workload of medical physicists or dosimetrists. We conclude that automated HVMAT can improve the current clinical practice allowing almost all breast cancer patients to have access to high-quality and standardized treatment.

Funding The authors received no specific financial support for the research, authorship, and/or publication of this article.

Author Contribution Concept: SC. Design: SC. Conduct: SC, CR, GM, FD, LS, LI Supervision: MB, LI, VV, AGM. Data acquisition: VEM, CR, LPDV. Statistical analysis: SC, MB. Critical review: VV, AGM. Manuscript drafting, editing: all authors. Revision and final approval: all authors.

Declarations

Conflict of interest S. Cilla, C. Romano, G. Macchia, M. Boccardi, L.P. De Vivo, V.E. Morabito, M. Buwenge, L. Strigari, L. Indovina, V. Valentini, F. Deodato and A.G. Morganti declare that they have no competing interests.

Ethical standards All procedures performed in studies involving human participants or on human tissue were in accordance with the ethical standards of the institutional and/or national research committee and with the 1975 Helsinki declaration and its later amendments or comparable ethical standards. The study received approval at the Gemelli Molise Hospital Institutional Review Board. Informed consent: not applicable; patients signed informed consent to the treatment procedure, but the study was retrospective.

References

1. Fisher B, Anderson S, Bryant J, Margolese RG, Deutsch M, Fisher ER et al (2002) Twenty-year follow-up of a randomised trial comparing total mastectomy, lumpectomy and lumpectomy plus irradiation for the treatment of invasive breast cancer. N Engl J Med 347:1233–1241. https://doi.org/10.1056/NEJMoa022152
2. Bartelink H, Horiot JC, Poortmans PM, Struikmans H, Van den Bogaert W, Fourquet A et al (2007) Impact of a higher radiation dose on local control and survival in breast-conserving therapy of early breast cancer: 10-year results of the randomized boost versus no boost EORTC 22881-10882 trial. J Clin Oncol 25(22):3259–3265. https://doi.org/10.1200/JCO.2007.11.4991
3. Immink JM, Putter H, Bartelink H, Cardoso JS, Cardoso MJ, van der Hulst-Vijgen MH et al (2012) Long-term cosmetic changes after breast-conserving treatment of patients with stage I–II breast cancer and included in the EORTC 'boost versus no boost' trial. Ann Oncol 23(10):2591–2598. https://doi.org/10.1093/annonc/mds066
4. Tortorelli G, Di Murro L, Barbarino R, Cicchetti S, Di Cristino D, Falco MD et al (2013) Standard or hypofractionated radiotherapy in the postoperative treatment of breast cancer: a retrospective analysis of acute skin toxicity and dose inhomogeneities. BMC Cancer 13:230. https://doi.org/10.1186/1471-2407-13-230
5. Borghero YO, Salehpour M, McNeese MD, Stovall M, Smith SA, Johnson J et al (2007) Multileaf field-in-field forward-planned in-

tensity-modulated dose compensation for whole-breast irradiation is associated with reduced contralateral breast dose: a phantom model comparison. Radiother Oncol 82:324–328. https://doi.org/10.1016/j.radonc.2006.10.011
6. Buwenge M, Cammelli S, Ammendolia I, Tolento G, Zamagni A, Arcelli A et al (2017) Intensity modulated radiation therapy for breast cancer: current perspectives. Breast Cancer (Dove Med Press) 9:121–126. https://doi.org/10.2147/BCTT.S113025
7. Guerrero M, Li XA, Earl MA, Sarfaraz M, Kiggundu E (2004) Simultaneous integrated boost for breast cancer using IMRT: a radiobiological and treatment planning study. Int J Radiat Oncol Biol Phys 59(5):1513–1522. https://doi.org/10.1016/j.ijrobp.2004.04.007
8. Hijal T, Fournier-Bidoz N, Castro-Pena P, Kirova YM, Zefkili S, Bollet MA et al (2010) Simultaneous integrated boost in breast conserving treatment of breast cancer: a dosimetric comparison of helical tomotherapy and three-dimensional conformal radiotherapy. Radiother Oncol 94(3):300–306. https://doi.org/10.1016/j.radonc.2009.12.043
9. Aly MM, Glatting G, Jahnke L, Wenz F, Abo-Madyan Y (2015) Comparison of breast simultaneous integrated boost (SIB) radiotherapy techniques. Radiat Oncol 10:139. https://doi.org/10.1186/s13014-015-0452-2
10. Corradini S, Ballhausen H, Weingandt H, Freislederer P, Schönecker S, Niyazi M et al (2018) Left-sided breast cancer and risks of secondary lung cancer and ischemic heart disease: effects of modern radiotherapy techniques. Strahlenther Onkol 194:196–205. https://doi.org/10.1007/s00066-017-1213-y
11. Badakhshi H, Kaul D, Nadobny J, Wille B, Sehouli J, Budach V (2013) Image-guided volumetric modulated arc therapy for breast cancer: a feasibility study and plan comparison with three-dimensional conformal and intensity-modulated radiotherapy. Br J Radiol 86:20130515. https://doi.org/10.1259/bjr.20130515
12. Fogliata A, Seppala J, Reggiori G, Lofefalo F, Palumbo V, De Rose F et al (2017) Dosimetric trade-offs in breast treatment with VMAT technique. Br J Radiol 90(1070):20160701. https://doi.org/10.1259/bjr.20160701
13. Balaji K, Balaji Subramanian S, Sathiya K et al (2020) Hybrid planning techniques for hypofractionated whole-breast irradiation using flattening filter-free beams. Strahlenther Onkol. https://doi.org/10.1007/s00066-019-01555-1
14. Bahrainy M, Kretschmer M, Jost V, Kasch A, Würschmidt F, Dahle J et al (2016) Treatment of breast cancer with simultaneous integrated boost in hybrid plan technique. Strahlenther Onkol 192(4):333–341. https://doi.org/10.1007/s00066-016-0960-5
15. Venjakob A, Oertel M, Hering DA, Moustakis C, Haverkamp U, Eich HT (2021) Hybrid volumetric modulated arc therapy for hypofractionated radiotherapy of breast cancer: a treatment planning study. Strahlenther Onkol 197(4):296–307. https://doi.org/10.1007/s00066-020-01696-8
16. Nelms BE, Robinson G, Markham J, Velasco K, Boyd S, Narayan S et al (2012) Variation in external beam treatment plan quality: an inter-institutional study of planners and planning systems. Pract Radiat Oncol 2:296–305. https://doi.org/10.1016/j.prro.2011.11.012
17. Zhao X, Kong D, Jozsef G, Chang J, Wong EK, Formenti SC et al (2012) Automated beam placement for breast radiotherapy using a support vector machine based algorithm. Med Phys 39:2536–2543. https://doi.org/10.1118/1.3700736
18. Mitchell RA, Wai P, Colgan R, Kirby AM, Donovan EM (2017) Improving the efficiency of breast radiotherapy treatment planning using a semiautomated approach. J Appl Clin Med Phys 18:18–24. https://doi.org/10.1002/acm2.12006
19. Kim H, Kwak J, Jung J, Jeong C, Yoon K, Lee S-W et al (2018) Automated field-in-field (FIF) plan framework combining scripting application programming interface and user-executed program for breast forward IMRT. Technol Cancer Res Treat 17:1533033818810391. https://doi.org/10.1177/1533033818810391
20. Cilla S, Ianiro A, Romano C, Deodato F, Macchia G, Buwenge M et al (2020) Template-based automation of treatment planning in advanced radiotherapy: a comprehensive dosimetric and clinical evaluation. Sci Rep 16:423. https://doi.org/10.1038/s41598-019-56966-y
21. Marrazzo L, Meattini I, Arilli C, Calusi S, Casati M, Talamonti C et al (2019) Auto-planning for VMAT accelerated partial breast irradiation. Radiother Oncol 132:85–92. https://doi.org/10.1016/j.radonc.2018.11.006
22. Cilla S, Macchia G, Romano C, Morabito VE, Boccardi M, Picardi V et al (2021) Challenges in lung and heart avoidance for post-mastectomy breast cancer radiotherapy: Is automated planning the answer? Med Dosim. https://doi.org/10.1016/j.meddos.2021.03.002
23. Chen K, Wei J, Ge C, Xia W, Shi Y, Wang H et al (2020) Application of autoplanning in radiotherapy for breast cancer after breast-conserving surgery. Sci Rep 10:10927. https://doi.org/10.1038/s41598-020-68035-w
24. Cilla S, Digesu C, Macchia G, Deodato F, Sallustio G, Piermattei A et al (2014) Clinical implications of different calculation algorithms in breast radiotherapy: a comparison between pencil beam and collapsed cone convolution. Phys Med 30(4):473–481. https://doi.org/10.1016/j.ejmp.2014.01.002
25. ICRU (2010) Report 83. Prescribing, recording, and reporting intensity-modulated photon-beam. J ICRU. https://doi.org/10.1093/jicru/10.1.report83
26. NSABP (2013) NSABP protocol B-51. mt-cancer.org/Protocols/B51_Protocol.pdf. Accessed 25 Apr 2014 (A randomized phase III clinical trial evaluating post-mastectomy chestwall and regional nodal xrt and post-lumpectomy regional nodal xrt in patients with positive axillary nodes before neoadjuvant chemotherapy who convert to pathologically negative axillary nodes after neoadjuvant chemotherapy)
27. Gagliardi G, Constine LS, Moiseenko V, Correa C, Pierce LJ, Allen AM et al (2010) Radiation dose-volume effects in the heart. Int J Radiat Oncol Biol Phys 76:77–85. https://doi.org/10.1016/j.ijrobp.2009.04.093
28. Lee BM, Chang JS, Kim SY, Keum K, Suh CO, Kim YB (2020) Hypofractionated radiotherapy dose scheme and application of new techniques are associated to a lower incidence of radiation pneumonitis in breast cancer patients. Front Oncol 10:124. https://doi.org/10.3389/fonc.2020.00124
29. Morganti AG, Cilla S, De Gaetano A, Panunzi S, Digesù C, Macchia G et al (2011) Forward planned intensity modulated radiotherapy (IMRT) for whole breast postoperative radiotherapy. Is it useful? When? J Appl Clin Med Phys 12:213e9. https://doi.org/10.1120/jacmp.v12i2.3451
30. Morganti AG, Cilla S, Valentini V, Digesù C, Macchia G, Deodato F et al (2009) Phase I–II studies on accelerated IMRT in breast carcinoma: technical comparison and acute toxicity in 332 patients. Radiother Oncol 90(1):86e92. https://doi.org/10.1016/j.radonc.2008.10.017
31. Van't Riet A, Mak AC, Moerland MA, Elders LH, van der Zee W (1997) A conformation number to quantify the degree of conformality in brachytherapy and external beam irradiation: application to the prostate. Int J Radiat Oncol Biol Phys 37:731–736. https://doi.org/10.1016/s0360-3016(96)00601-3
32. Cilla S, Deodato F, Digesù C, Macchia G, Picardi V, Ferro M et al (2014) Assessing the feasibility of volumetric-modulated arc therapy using simultaneous integrated boost (SIB-VMAT): an analysis for complex head-neck, high-risk prostate and rectal cancer cases. Med Dosim 39(1):108–116. https://doi.org/10.1016/j.meddos.2013.11.001

33. Abo-Madyan Y, Aziz MH, Aly MMOM, Schneider F, Sperk E, Clausen S et al (2014) Second cancer risk afer 3D-CRT, IMRT and VMAT for breast cancer. Radiother Oncol 110:471–476. https://doi.org/10.1016/j.radonc.2013.12.002
34. Macchia G, Cilla S, Buwenge M et al (2020) Intensity-modulated radiotherapy with concomitant boost after breast conserving surgery: a phase I–II trial. Breast Cancer 12:243–249. https://doi.org/10.2147/BCTT.S261587
35. Vrieling C, Collette L, Fourquet A, Hoogenraad WJ, Horiot JC, Jager JJ et al (1999) The influence of the boost in breast conserving therapy on cosmetic outcome in the EORTC "boost versus no boost" trial. Int J Radiat Oncol Biol Phys 45:677–685. https://doi.org/10.1016/s0360-3016(99)00211-4
36. Pignol JP, Olivotto I, Rakovitch E, Gardner S, Sixel K, Beckhamet W et al (2008) A multicenter randomized trial of breast intensity-modulated radiation therapy to reduce acute radiation dermatitis. J Clin Oncol 26:2085–2092. https://doi.org/10.1200/JCO.2007.15.2488
37. Stovall M, Smith SA, Langholz BM, Boice JD Jr, Shore RE, Andersson M et al (2008) Dose to the contralateral breast from radiotherapy and risk of second primary breast cancer in the WECARE study. Int J Radiat Oncol Biol Phys 72:1021–1030. https://doi.org/10.1016/j.ijrobp.2008.02.040
38. Grantzau T, Thomsen MS, Vaeth M, Overgaard J (2014) Risk of second primary lung cancer in women after radiotherapy for breast cancer. Radiother Oncol 111(3):366–373. https://doi.org/10.1016/j.radonc.2014.05.004
39. Asakura H, Hashimoto T, Zenda S, Harada H, Hirakawa K, Mizumoto M et al (2010) Analysis of dose-volume histogram parameters for radiation pneumonitis after definitive concurrent chemoradiotherapy for esophageal cancer. Radiother Oncol 95(2):240–244. https://doi.org/10.1016/j.radonc.2010.02.006
40. Darby SC, Ewertz M, McGale P, Bennet AM, Blom-Goldman U, Brønnum D et al (2013) Risk of ischemic heart disease in women after radiotherapy for breast cancer. N Engl J Med 368:987–998. https://doi.org/10.1056/NEJMoa1209825
41. Viren T, Heikkila J, Myllyoja K, Koskela K, Lahtinen T, Seppala J (2015) Tangential volumetric modulated arc therapy technique for left-sided breast cancer radiotherapy. Radiat Oncol 10:79. https://doi.org/10.1186/s13014-015-0392-x
42. van Mourik A, van Kranen S, den Hollander S, Sonke JJ, van Herk M, van Vliet-Vroegindeweij C (2011) Effects of setup errors and shape changes on breast radiotherapy. Int J Radiat Oncol Biol Phys 79:1557–1564. https://doi.org/10.1016/j.ijrobp.2010.07.032
43. Lizondo M, Latorre-Musoll A, Ribas M, Carrasco P, Espinosa N et al (2019) Pseudo skin flash on VMAT in breast radiotherapy: optimization of virtual bolus thickness and HU values. Phys Med 63:56–62. https://doi.org/10.1016/j.ejmp.2019.05.010
44. Reitz D, Walter F, Schönecker S, Freislederer P, Pazos M, Niyazi M et al (2020) Stability and reproducibility of 6013 deep inspiration breath-holds in left-sided breast cancer. Radiat Oncol 15(1):121. https://doi.org/10.1186/s13014-020-01572-w
45. Piroth MD, Baumann R, Budach W, Dunst J, Feyer P et al (2018) Heart toxicity from breast cancer radiotherapy. Strahlenther Onkol 195(1):1–12. https://doi.org/10.1007/s00066-018-1378-z
46. Fogliata A, Vanetti E, Clivio A, Nicolini G, Winkler P, Cozzi L (2006) The impact of photon dose calculation algorithms on lung tissue under different respiratory phases. Phys Med Biol 51:142138. https://doi.org/10.1088/0031-9155/53/9/011